KSME Journal, Vol. 2, No. 1, pp. 19~27, 1988.

A STUDY ON THE CHARACTERISTICS OF HEAT TRANSFER IN AN ENGINE PISTON

H. W. Wu* and C. P. Chiu*

(*Received January 11, 1988*)

The piston temperature distribution with varying engine torque and speeds for a real engine operation has been determined by a numerical model. The model is developed by the finite element conduction method combined with engine simulation. In this model, the two boundary temperature concept instead of one constant boundary temperature was presented to approximate the ambient temperatures along the piston skirt. The two temperatures were first estimated, then adjusted by the iterated process, for predicting piston temperatures, according to the energy balance of the whole engine energy system. In order to verify the predicted values, input data for cycle simulation were obtained, the piston temperatures were also measured. In this way the good agreement between the model and experimental results could be checked.

Key Words: Heat Transfer, Engine Piston, Temperature Distribution

NOMENCLATURE

A : Area
C_p : Specific heat capacity
D : Cylinder bore
F : Equivalence ratio
f : Fuel-air ratio
H : Enthalpy
h : Heat transfer coefficient
I : Functional
K : Conductivity
$[K]$: Heat transfer conduction matrix
k : Specific heat capacity ratio
M : Mass
P : Pressure
$\vec{P}$: A vector of applied heat flow on the surface
P_r : Prandtl number
$\Sigma\dot{Q}$: Sum of heat transfer rate
R : Gas constant
R_e : Reynolds number
T : Temperature
$\vec{T}$: A vector of temperature at grid points
T_p : Piston temperature calculated by cycle simulation
T_p^* : Area-averaged piston crown temperature computed by finite element model
U : Internal energy
V : Volume
V_p : Mean piston velocity
X : Heat transfer path
θ : Crank angle
ρ : Density

Superscripts

$\cdot$: Differential w.r.t. time
$\bar{}$: Mean w.r.t. time

Subscripts

C : Coolant
E : Exhaust port
F : Fuel
g : Gas
I : Inlet port
in : Entering system
out : Leaving system
S : Stoichiometric

*Department of Mechanical Engineering, National Cheng Kung University, Tainan, Taiwan, R.O.C.

1. INTRODUCTION

In recent years there has been a growing need to increase the number of diesel engines used in passenger cars and agricultural machines, in order to obtain higher specific power output. However, it was found that piston cracking in diesel engines occurred more often. It is not known whether the piston cracking was caused by poor cooling at the higher engine speed or load (Horng Wen Wu, 1981). In order to identify the cause, the heat transfer in the piston must be studied. Generally, the combustion chamber gas temperature and heat transfer coefficient of the cylinder wall have pronounced effect on the temperature distribution in the piston. The gas temperature, pressure, and composition in the cylinder can be obtained from a cycle simulation (Mattavi and Amann, 1978) of the engine such as thermodynamic anlysis models (Borman et al, 1972), phenomenological models (Dent and Mehta, 1981) and multidimensional models (Bulter et al, 1982).

The calculations associated with phenomenological models and multidimensional models are formidable and the computer costs are currently prohibitive. The thermodynamic simulation model of the engine cycle is the one chosen for this study. It can predict the thermodynamic characteristics of engine operating conditions with sufficient accuracy. It offers the necessary information for the calculation of piston tem-

perature. Regarding investigations on the temperature of pistons in automotive engines with experimental measurement, there have been many reports (Furuhama and Enomoto, 1973; Kruggle, Otto, 1971; Procknow, 1978; Yoshida, 1983; Takahisa et al, 1983). Furuhama (1973) and Yoshida (1983) have made the most pertinent experiments for our use among the investigators cited. They have studied the correlations between engine speed, equivalence ratio and temperature distribution of the piston with different engines and different operating conditions. In recent years, finite element method has been used to calculate piston temperature (Procknow, 1978; Takahisa, et al, 1983; Chin Hsiu Li, 1982; Wallance, et al, 1983). Of the investigators cited above, none of them have addressed the idea of the piston thermal system considered as one part of the engine energy system. We, in our studies, have developed a piston thermal system model from which numerical piston temperature values for gasoline engines can be computed (C. P. Chiu, et al, 1984). In this paper, the gas pressure, gas temperature and gas-side heat transfer coefficients were obtained from thermodynamics cycle simulation by considering the balance of the heat flow rate over the full cycle against the heat flow rate through the metal components to modify the assumed metal walls temperatures. Furthermore, the temperature distribution of the piston was analyzed by an axi-symmetrical finite element conduction model under various engine speeds and torque operating conditions. In addition, we address the variations of piston temperature with change in gas-side heat transfer coefficients and gas temperature respectively. One important use of thermodynamics cycle simulation is in conjunction with experiments where cylinder pressure was recorded as a function of crank angle over a wide range of engine operating conditions. For verification, the temperatures of pistons were experimentally measured with thermocouples. A special linkage mechanism was designed to connect the thermocouple lead wires to the recorder.

2. CYCLE SIMULATION FOR AN ENGINE

2.1 Calculation of Gas Temperature and Heat Transfer Coefficients

This analysis is based on the concept that the piston thermal system is considered to be one part of the whole energy engine system. So the current cycle simulation is intended to obtain gas temperature and gas-side heat transfer coefficient for the predicted piston temperature and temperature distribution in the piston. Throughout the cycle, the cylinder is treated as a variable volume plenum, spatially uniform in pressure. The gas components are subjected to obey the ideal gas laws. The engine system is subdivided in three parts, engine cylinder, intake and exhaust ports. The fundamental equations may be written as follows.

Conservation of mass

$$\dot{M}=\dot{M}_{in}-\dot{M}_{out} \tag{1}$$

Conservation of energy—apply to an open transient system

$$\frac{d(MU)}{dt}=\Sigma\dot{Q}-\frac{P\dot{V}}{J}+\dot{M}_{in}-\dot{M}_{out}\ H_{out} \tag{2}$$

General heat transfer equation

The heat transfer model used for each of the five surfaces is taken to be equivalent to one-dimensional.

$$Q_{in}=\frac{T_g-T_c}{\frac{1}{h_gA_g}+\frac{X_w}{K_wA_w}+\frac{1}{h_cA_c}} \tag{3}$$

h_g denotes the heat transfer coefficient between the burned gas and walls which can be estimated by a number of empirical correlations (Eichelberg, 1939; Annand, 1963; Woschni, 1967). The empirical relation used here is proposed by Annand (1963), but with the radiation effect additionally incorporated. The resulting relationship is:

$$h_g=2.4\times10^{-4}\ \frac{K_0^{1-b}}{D}\left(\frac{T}{T_0}\right)^{0.8(1-b)}\left(\frac{\rho C_p V_p D}{P_r}\right)^b +\sigma\cdot\alpha(1-e^{-\lambda L})\ \frac{T_w^4-T^4}{T_w-T} \tag{4}$$

where

$P_r=0.7,\ b=0.75$
$K_0=0.0301\text{W/m}\cdot{}^\circ\text{K}$
$T_0=366.7^\circ\text{K}$
σ = Stefan−Boltzman constant
$=5.678\times10^{-8}\text{W/m}^2\cdot{}^\circ\text{K}$
α = 0.9 for head and piston
= 0.25 for sleeve
λ = designates emitted soot number per unit path length
$=2.185\cdot\rho\cdot f/1+f$
L = bore, for the sleeve
= instantaneous distance from piston to head, for head and piston.

h_0 is the heat transfer coefficient of coolant, Dittus and Boelter correlation (Dittus and Boelter, 1930) is adopted for this study since it considers turbulent forced convection heat transfer.

$$h_0=0.023\ (R_e)^{0.8}\ (P_r)^{0.4} \tag{5}$$

Equivalence ratio

Equivalence ratio is defined as the ratio of actual fuel-air ratio to stoichiometric fuel-air ratio. Neglecting blowby, the equation for equivalence ratio (Borman, et al, 1972) is

$$F=\frac{\frac{M_oF_o}{1+f_0}\int_0^t\left(\frac{\dot{M}_IF_I}{1+f_I}+\frac{\dot{M}_EE_E}{1+f_E}+\frac{\dot{M}_F}{f_S}\right)dt}{\frac{M_0}{1+f_0}\int_0^t\left(\frac{\dot{M}_I}{1+f_I}+\frac{\dot{M}_E}{1+f_E}\right)dt} \tag{6}$$

The mass ratio of intake and exhaust process

The process is considered to be isentropic steady flow.

$$\dot{M}_v=AP_0\sqrt{\frac{g_c}{R_0T_0}\cdot\frac{2k}{k-1}\left[\left(\frac{P}{P_0}\right)^{\frac{2}{k}}-\left(\frac{P}{P_0}\right)^{\frac{k+1}{k}}\right]} \tag{7}$$

Simplification of the above equations results in the derivative

$$\dot{T}=\frac{B-\frac{P}{A}\frac{\partial U}{\partial P}\frac{\dot{M}}{M}-\frac{\dot{V}}{V}+\frac{\partial R}{\partial F}\frac{\dot{F}}{R}-\frac{\partial U}{\partial F}\dot{F}}{\frac{\partial U}{\partial T}+\frac{\partial U}{\partial P}\frac{P}{T}\frac{C}{A}} \tag{8}$$

where

$$A=1-\frac{P}{R}\frac{\partial R}{\partial P}$$

$$B=(-P\dot{V}+\Sigma\dot{Q}+\dot{M}_{in}H_{in}-\dot{M}_{out}H_{out}-\dot{M}U)\left(\frac{1}{M}\right)$$

$$C=1+\frac{T}{R}\cdot\frac{\partial R}{\partial T}$$

2.2 Heat Release During Combustion

Heat release rates during combustion are predicted from experimentally obtained engine pressure-time data. With two zone combustion model (Horng Wen Wu, 1981) such data can be used to derive mass-fraction burned as a function of crank angle. The resulting mass burned curve can then be used in the cycle simulation program.

3. FINITE-ELEMENT MODEL APPLIED TO PREDICTING PISTON TEMPERATURE DISTRIBUTION

Before the governing equations are presented, the following assumptions were adopted,

(a) Piston has an axially symmetric geometry.

(b) The conductivity K of piston is constant.

(c) This model is used to account only for steady-state analysis. It ignores the change of gas temperature and heat-transfer coefficients that occur during the combustion cycle. The time-mean gas temperature and heat-transfer coefficients were utilized.

3.1 Governing Equations

The heat conduction equation in cylindrical coordinate for an axi-symmetric field is

$$K\left(\frac{1}{r}\frac{\partial T}{\partial r}+\frac{\partial^2 T}{\partial r^2}\right)+k\frac{\partial^2 T}{\partial z^2}=0 \tag{9}$$

The gas-side heat transfer equation of the piston crown is

$$K\left(\frac{\partial T}{\partial n}\right)_w=h_g(T_g-T) \tag{10}$$

where $\bar{h}_g$ and $\overline{T}_g$ denote mean value throughout the cycle. i.e.

$$\bar{h}_g=\frac{1}{4\pi}\int_0^{4\pi}h_g d\theta \tag{11}$$

$$\overline{T}_g=\frac{1}{4\pi\bar{h}_g}\int_0^{4\pi}T_g h_g d\theta \tag{12}$$

where h_g and T_g are functions of crank angle, h_g is computed by Eq. (4), with the data from cycle simulation.

The heat transfer equations associated with various cooled surfaces are

$$K\left(\frac{\partial T}{\partial n}\right)_a=h_a(T_{a,\,a}-T) \tag{13}$$

where α denotes the various heat transfer surfaces.

a denotes ambient side of the surfaces.

The formulation of this finite element model and a method of solution are described below.

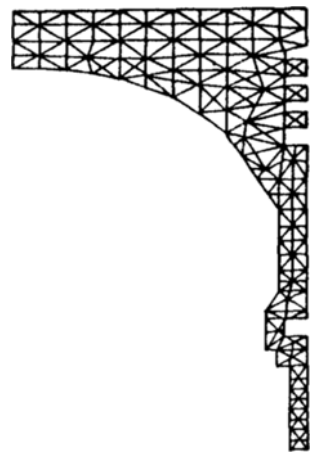

Fig. 1 The element distribution plot with 172 nodes and 247 elements.

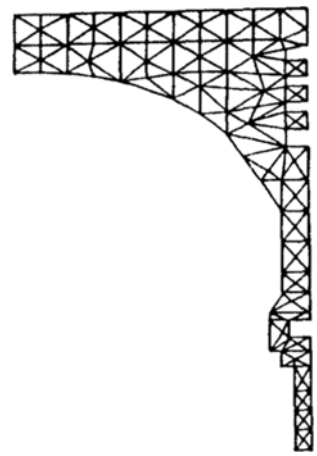

Fig. 2 The element distribution plot with 119 nodes and 166 elements.

$$I=\frac{1}{2}\int_z\int_r K\left[\left(\frac{\partial T}{\partial Z}\right)^2+\left(\frac{\partial T}{\partial r}\right)^2\right]rdrdz+\frac{1}{2}\int_{Ba}h(T-T_a)^2rdr \tag{14}$$

Half a spatial domain was discretized with 172 nodes and 247 elements as shown in Fig. 1, treating the whole piston by axi-symmetry. Similarly, it was also discretized with 119 nodes and 166 elements as illustrated in Fig. 2. But the results, calculated with each mesh, were not so much differênt. Hence the latter mesh was used to calculate the temperature distribution for all operating conditions. The matrix form could thus be obtained (Procknow, 1978).

$$(K)\vec{T}=\vec{P} \tag{15}$$

3.2 Boundary Conditions

The most difficult task in implementing any conduction heat transfer model may be the application of the appropriate boundary conditions, such as gas temperature, gas-side heat transfer coefficient, gas wall-side heat transfer coefficients and wall-side ambient temperatures.

The gas temperature and gas-side heat transfer coefficients during various operating conditions are obtained from the thermo-dynamics cycle simulation. It is difficult to measure

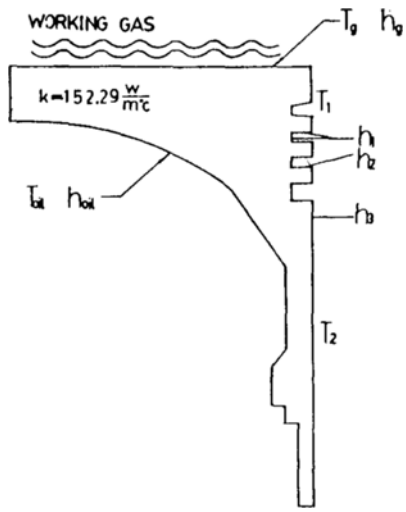

Fig. 3 Schematic representation piston thermal system

the wall-side heat transfer coefficients which exist in the piston ring groove and underside of the piston. The data of Pachernegg (1967) and Li (1982) were used as a guide for the selection of these coefficients.

It was cited by Pachernegg that a heat transfer coefficient between piston skirt and cylinder wall was between 284 and 483 $W/m^2 \cdot °K$. The heat transfer coefficient in the top ring groove was between 568 and 79.4$W/m^2 \cdot °K$, and a value between 56.7 and 79.4 $W/m^2 \cdot °K$, was used along the piston under-side. Li calculated the piston temperature distribution based on a value of 150 $W/m^2 \cdot °K$ between the skirt and cylinder wall, 800 $W/m^2 \cdot °K$ in the top ring groove, 1000$W/m^2 \cdot °K$ in the bottom ring groove and 49.9$W/m^2 \cdot °K$ along the piston under-side, and so on. Hence in this paper, the heat transfer coefficients are as follows (see Fig. 3).

$h_1 = 650 W/m^2 \cdot °K$
$h_2 = 1000 W/m^2 \cdot °K$
$h_3 = 150 W/m^2 \cdot °K$

Li (1982) selected only one ambient temperature for the outer surface of the piston and considered it as constant for various operating conditions. But to account for the temperature distribution, a constant temperature seemed to be unreasonable, so we choose two temperatures to approximate the ambient temperatures and considered them as variable over various operating states. Because the top ring groove was affected more by the cylinder gas, we selected the temperature from the piston crown to first ring land as T_1 (the higher temperature) and T_2 the rest. The temperature T_1 and T_2 were first estimated, then adjusted after each computation was made, until the piston crown area-averaged temperature was equal to piston temperature calculated from the cycle simulation. However, the final values for T_1 and T_2 must be adjusted concurrently, so that the obtained isothermal lines are reasonable parallel. The flow diagram used for the iterated process was shown in Fig. 4. For the surfaces of piston under-side, the oil temperature toil was measured directly from experiment.

3.3 Computation Flow Diagram

Figure 4 illustrates the computation flow diagram of piston temperature distribution. The data of the whole program, such as engine geometry, fuel consumption, gas pressure-time

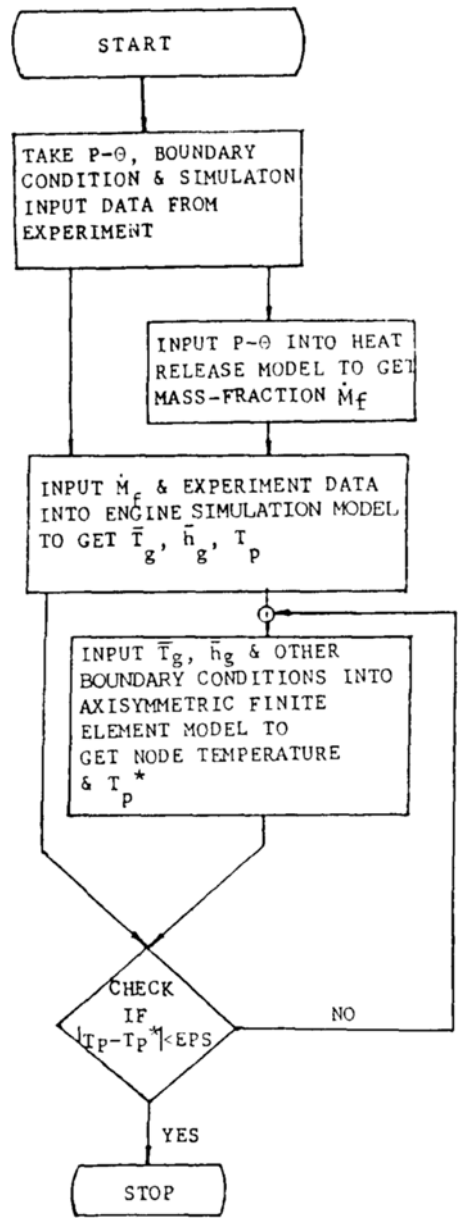

Fig. 4 Computation flow diagram of piston temperature distribution

history, cooling system temperature and so on, were obtained by measurement. The mass-fraction burned $\dot{m}_f$ was first calculated from the engine pressure-time data by the heat release model. Then, the thermodynamic cycle simulation, which used engine geometry, fuel consumption, mass-fraction burned, cooling system characteristics etc., calculated gas conditions in the combustion chamber as a function of the crank angle, and the mean value of gas conditions were also obtained. Finally, the finite element model utilized the output from the thermodynamic cycle simulation, together with data related to engine geometry, metal properties, and cooling system characteristics.

4. EXPERIMENTAL EQUIPMENT AND METHOD

The test engine was a ER17 farm diesel engine of new

Table 1 Major specifications of engine

Cylinder number	1
Stroke	95 mm
Bore	110 mm
Connecting rod length	168±0.125 mm
Displacement	902 c.c.
Injection timing	19 BTDC
Inlet valve opening	20 BTDC
Inlet valve closing	45 ABDC
Exhaust valve opening	50 BBDC
Exhaust valve closing	15 ATDC
Cooling system	Water
Rated power and speed	9.43 kW and 2000 rpm
Intake system	Naturally aspirated

Taiwan Agricultural Machine Manufacture Company. The major specifications of the engine tested are shown in Table 1. The pressure-crank angle data, oil temperature, cooling water temperature and fuel consumption etc. were obtained at various engine speeds (800, 1000, 1200, 1600, 2000, 2200 rpm) and engine torques (0, 10, 20, 30, 40 N-m) respectively. Furthermore, the engine was tested at maximum power, rated power and maximum torque respectively. The experimental rig and equipment were as shown in Fig. 5. The designed linkage mechanism (Furuhama, 1973) utilized is shown in Fig. 6, with guiding thermocouples to measure piston temperature. Thermocouples used were OMEGA TECH-0.05″, TFCR-0.05″ thermocouples with the advantages of small diameter and flexibility.

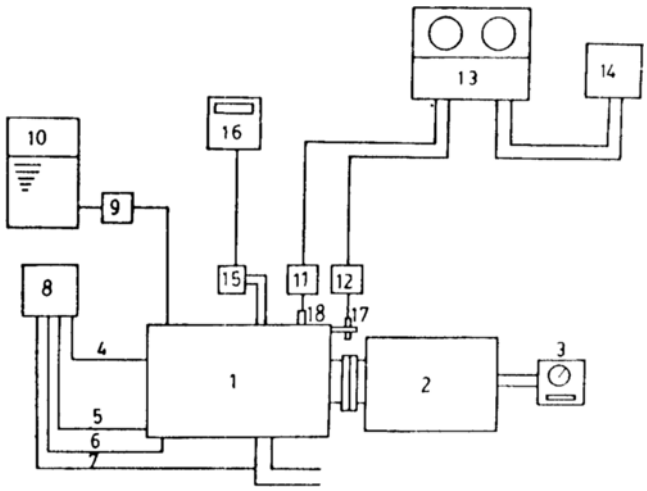

1. Test engine
2. D. C. dynamometer
3. Tachometer
4. 5, 6, 7. Thermocouples
8. Multi-channel temperature recorder with indicator
9. Flow meter for liquid fuel
10. Tank for liquid fuel
11. Charge amplifier
12. Degree marker amplifier
13. TEAC analog data recorder
14. Oscilloscope
15. Air flow meter
16. Digital indicator for air flow
17. Degree marker sensor
18. Piezo electric pressure transducer.

Fig. 5 Schematic diagram of experimental apparatus

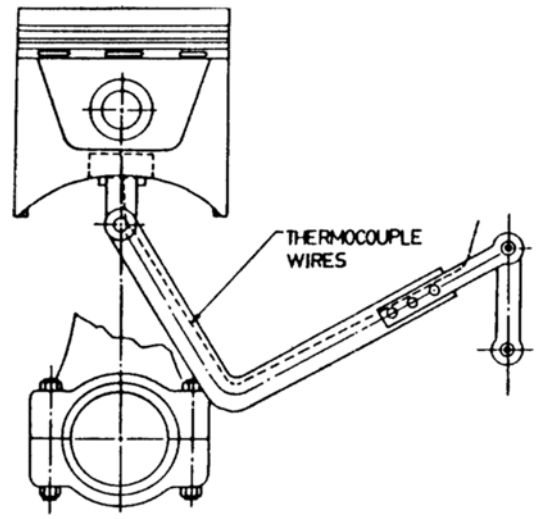

Fig. 6 Piston with linkage mechanism for guiding thermocouple wires

5. RESULTS AND DISCUSSIONS

The characteristics of gas pressure, gas temperature and gas-side heat transfer coefficient versus crank angle calculated from cycle simulation were as shown in Fig. 7 and Fig. 8 respectively. In this paper, the mean values throughout the entire cycle were taken from the calculated values for the calculations of piston temperature distributions. Fig. 9 and Fig. 10 illustrate the temperature distributions of piston calculated by the finite element model. The temperature trend shows a gradual increase along the piston under-side toward the piston crown, and from the edge toward the center also.

These temperature trends agree with the experimentally measured results as shown in Fig. 11 and Fig. 12. Both show that the temperature of the piston crown center was the highest in the piston. The comparison of the simulated and measured temperature values illustrates that the model and boundary conditions adopted are reasonable. Fig. 13 and Fig.

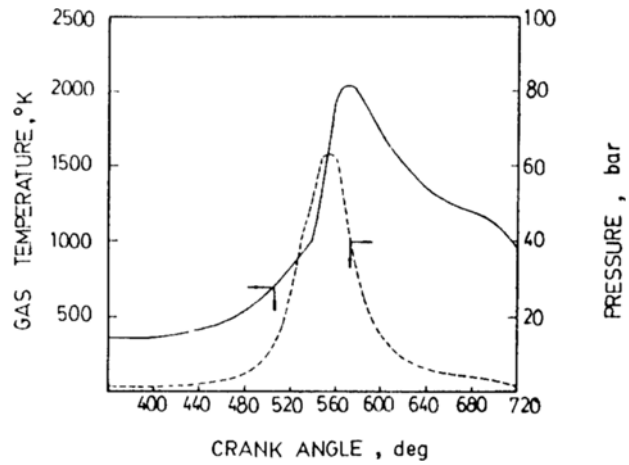

Fig. 7 Correlations between gas pressure, temperature and crank angle at engine speed 800 rpm, torque 40N-m.

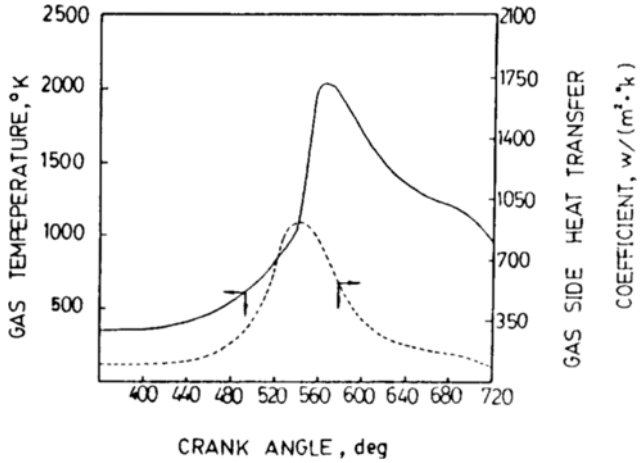

Fig. 8 Correlations between gas temperature, gas-side heat transfer coefficient and crank angle at engine speed 800 rpm, torque 40N-m.

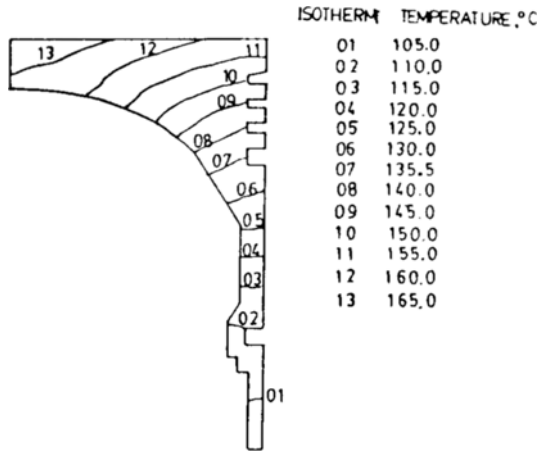

Fig. 9 The temperature distribution of piston at 1600 rpm, 10N-m.

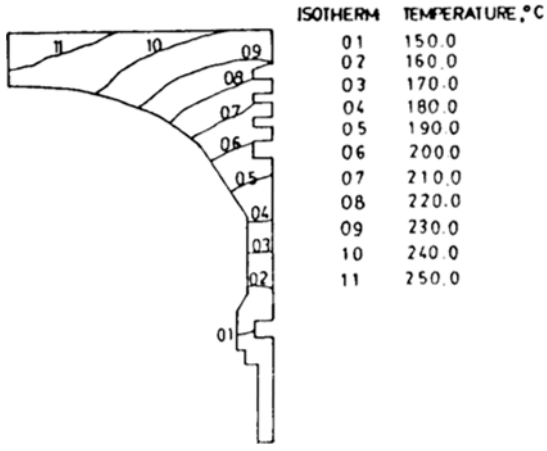

Fig. 10 The temperature distribution of piston at 1600 rpm, 40 N-m.

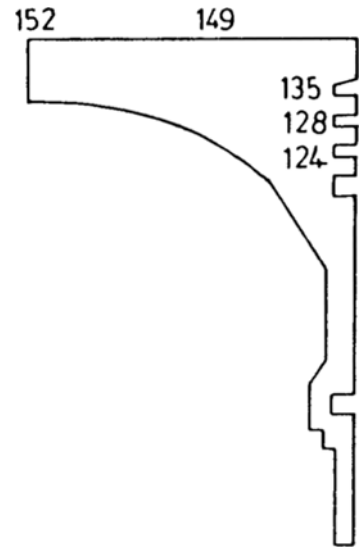

Fig. 11 The piston temperature (℃) measured at 1600 rpm, 10N-m.

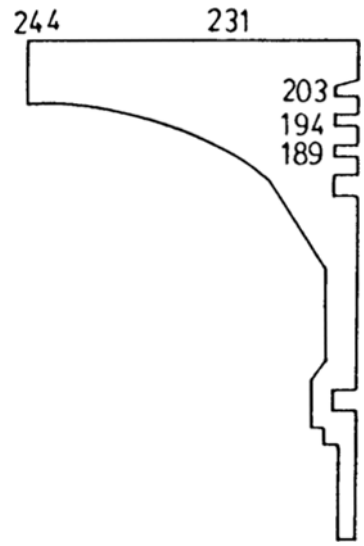

Fig. 12 The piston temperature measured at 1600 rpm, 40 N-m.

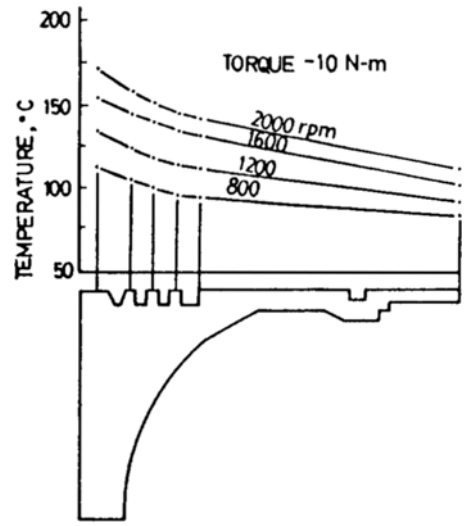

Fig. 13 The variations of ring temperature with different engine speed, at 10N-m

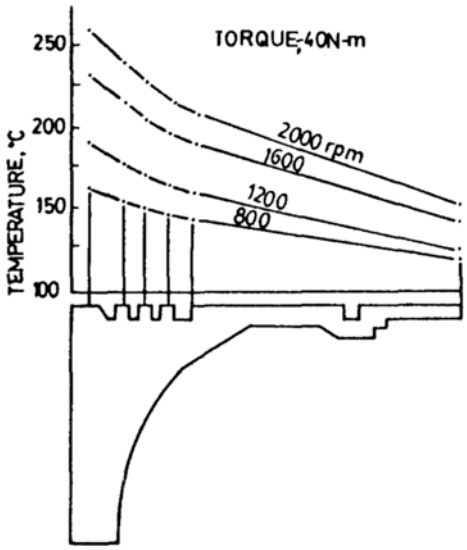

Fig. 14 The variations of ring temperature with different engine speed, at 40N-m

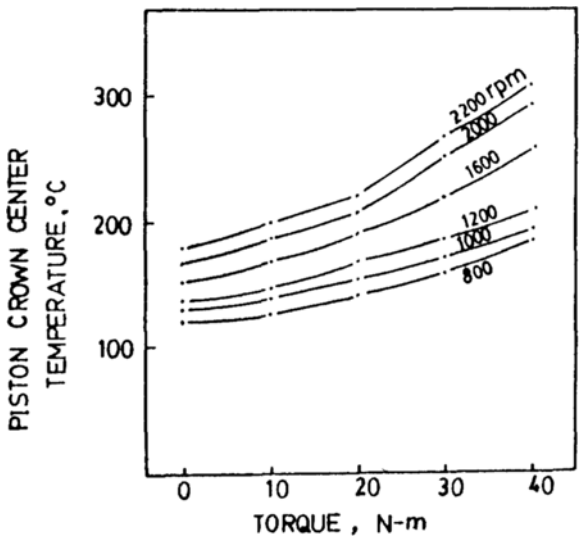

Fig. 15 The correlation of temperature at piston crown center and engine torque with various engine speed

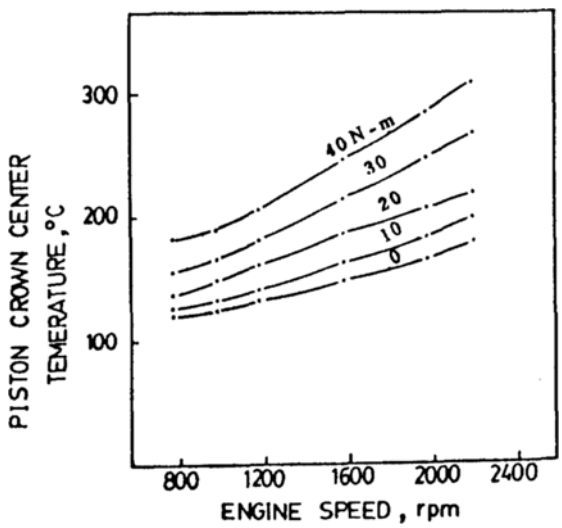

Fig. 16 The correlation of temperature at piston crown center with engine speed at various torque

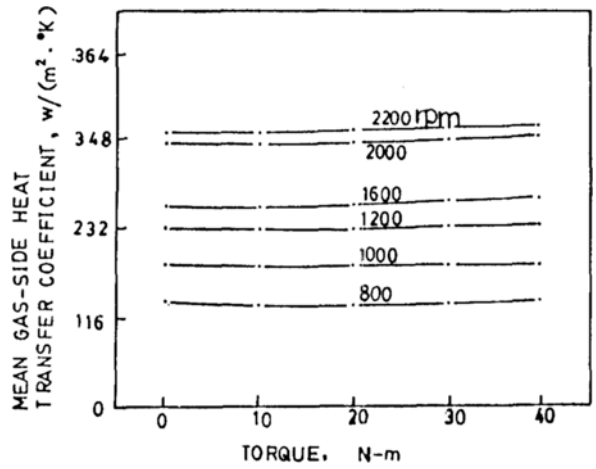

Fig. 17 Variations of mean gas-side heat transfer coefficient with engine torque at various engine speed

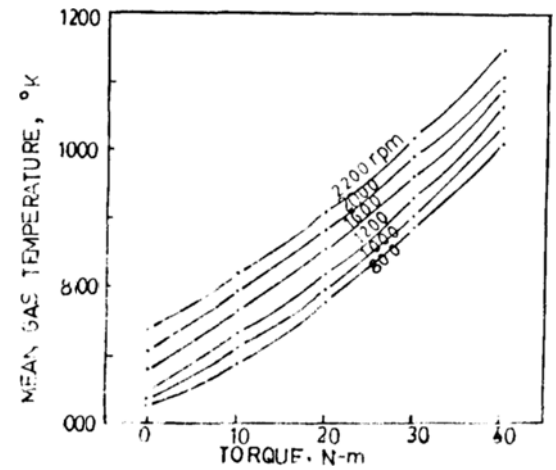

Fig. 18 Variations of mean gas temperature with engine torque at various speed

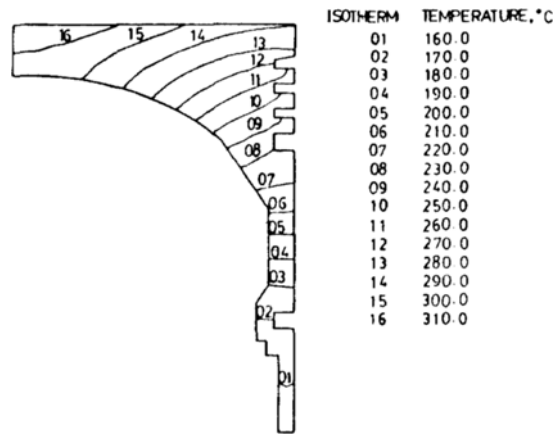

Fig. 19 The piston temperature distribution at rated power operating state (9.43KW/2000rpm)

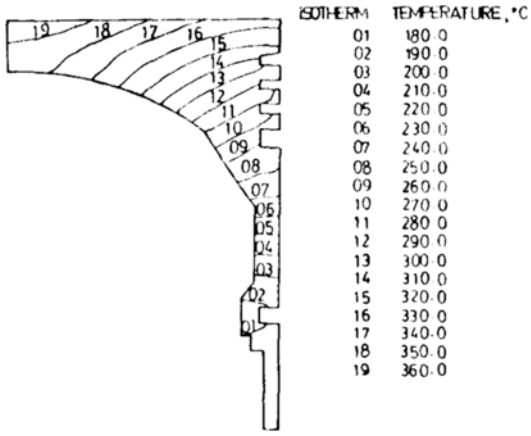

Fig. 20 The piston temperature distribution at maximum power operating state (10.21 KW/2000rpm)

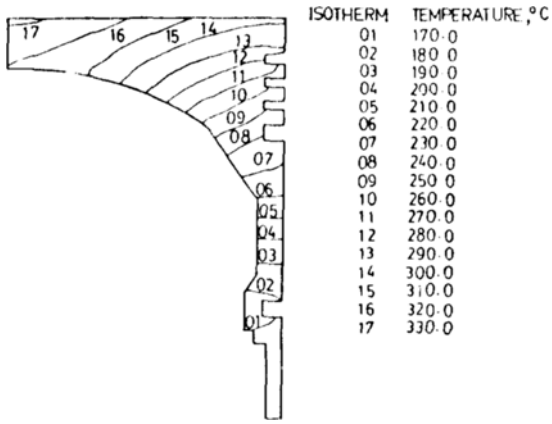

Fig. 21 The piston temperature distribution at maximum torque operating state (52 N-m/1600 rpm)

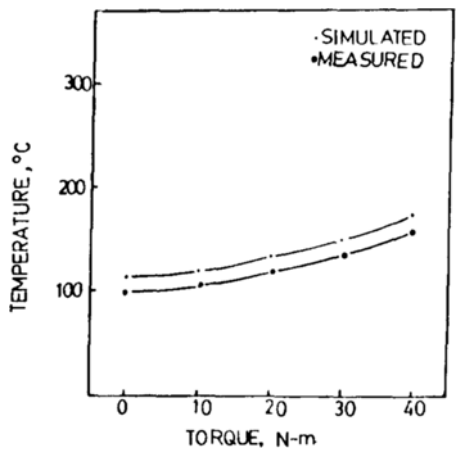

Fig. 22 The comparison of experiment and calculated results with different torque at engine speed 800 rpm

14, show the temperature distribution in the piston skirt. It shows that the temperature decrease at the ring belt was very large, and that the ring is quite important for cooling the piston. It was found that in general the designing of piston for the prevention of piston cracking depends on the location, dimensions and variety of the piston ring.

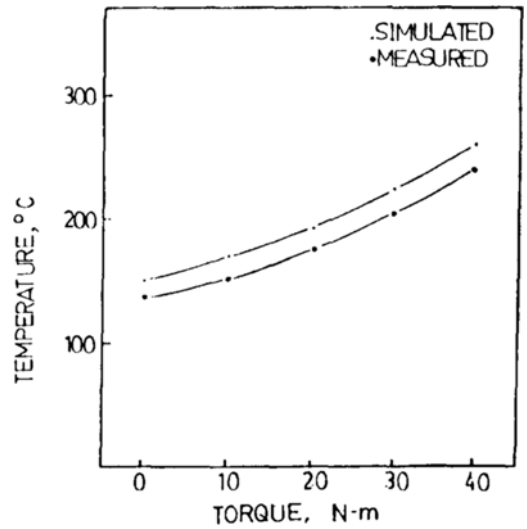

Fig. 23 The comparison of experiment and calculated results with different torque at engine speed 1600rpm

The correlation of temperature at the piston crown center with engine load is shown in Fig. 15. It shows that the temperature increases with engine torgue. The reason for the trend might be explained from studying Fig. 17 and Fig. 18. Fig. 17 shows that the mean gas-side heat transfer coefficient does not change with increasing torque at same speed, but Fig. 18 shows that the gas temperature increased with increasing heat release rate, due to more fuel per cycle. The temperature at the piston crown center also increased as engine spped increased, as shown in Fig. 16. These results could be explained from Fig. 17 and Fig. 18. In Fig. 17 the heat transfer coefficient increased as fluid flow accelerated at higher engine speeds. That is, the increasing heat transfer rate to piston and increasing gas side temperature as shown in Fig. 18 resulted in the higher piston temperature.

The temperature variations at the maximum power, rating power and maximum torque state are as shown from Fig. 19 to Fig. 21 respectively. It might be observed that the maximum temperature occurred at the maximum power state.

The comparison of experiment and calculated results are shown in Fig. 22 and Fig. 23. Both curves have the same trend with torque. The result of the predicted value of piston temperature agreeing fairly closely with the measured value gives one coincidence in the use of simulation model. One of the reasons causing the deviation is the uncertainty of boundary conditions at coolant sides.

6. CONCLUSION

This paper has presented a numerical model on the temperatures prediction of piston imposed by thermal loading under real engine operating conditions. The results can be summarized as follows:

(1) The results showed that heat transfer rate increased with increasing engine speed, and also with increasing, engine torque resulting from increasing heat release amount. Both these characteristics increased the piston temperature.

(2) The temperature decreased at the ring belt was very large, and it might be concluded that the heat flow from the rings and ring lands to the cylinder wall was very large.

(3) The maximum temperature existed at the maximum power state, and the temperature reached at the maximum torque point was lower.
(4) A comparison of calculated and experimental results showed that they have reasonable coincidence. In order to improve the accuracy, we must have more measurement on the related boundary conditions.

ACKNOWLEDGEMENT

The authors wishe to express their gratitude to the New Taiwan Agriculture Machine Manufacture Company for experimental assistance for this study.

REFERENCES

Annand W. J. D., 1963, "Heat Transfer in the Cylinders of Reciprocating Internal Combustion Engines", Proc. Inst. Mech. Engrs. Vol. 177, No. 36, p. 973.

Borman G. L., Myers P. S., Uyehara O.A., 1972, "Engine Simulation Studies", Technical Report No. 11398, The University of Wisconsin, March.

Butler T. D., Coloutman L. D., Dukowicz J. K., and Ramshaw J. D., 1982, "Multidimensional Numerical Simulation of Reactive Flow in Internal Combustion Engines", Progress in Energy and Combustion Science, Vol. 7.

C. P. Chiu H. W.Wu and C. T. Ju, 1984, "Numerical Solution for Piston Temperature Distribution in a Gasoline Engine", Proceedings of 4th International Conference in Applied Numerical Modeling, p. 620, December.

Chin Hsiu Li, 1982, "Piston Thermal Deformation and Friction Consideration"s, SAE Paper 820086.

Dent J. C. and Mehta Pramod S., 1981, "Phenomenological Combustion Mode for a Quiescent Chamber Diesel Engine", SAE Paper 811235.

Dittus, F. W. and Boelter L. M. K., 1930,: Univ. Calif. (Berkerley) Pub. Eng., Vol. 2, p. 443.

Eichelberg, G., 1939, "Investigations on Combustion Engines Problems", Engineering, Vol. 148.

Furuhama Shoichi and Enomoto Yoshiteru, 1973, "Piston Temperature of Automobile Gasoline Engine in Driving on the Road, "Bulletin of JSME, Vol, 16, No. 99. Sep., 1973.

Horng Wen Wu, 1981, "Instantaneous Heat Transfer Rates to the Cylinder Head Surface of a Farm Diesel Engine", M. S. Thesis of M. E. Department, Cheong Kung University, R.O.C., May.

Kruggle Otto, 1971, "Calculation and Measuring of Piston Temperature of Air Cooled Two Stroke Gasoline Engines", SAE Paper 7110578.

Mattavi James N. and Amann Charles A., 1978. "Combustion Modeling in Reciprocating Engine", Proceeding of the Symposium on Combustion Modeling in Reciprocating Engines, held at General Motors Research Laboratories, Warren, Michigan, November 6th and 7th.

Pachernegg S. I., 1967, "Heat Flow in Engine Pistons", SAE Paper 670928.

Procknow David William, 1978, "Calculation and Measurement of Piston Temperature in a Water-Cooled Two-Stroke Cycle Gasoline Engine", M. S. Thesis, M. E. Department, University of Wisconsin, Madison.

Takahisa Hasebe et. al, 1983, "Thermal Measurement and Analysis of Engine Components-Part I, Measurement and Analysis of Piston", Transaction of the Society of Automotive Engineers of Japan, No. 27, 55.

Wallace F. J., Kao T. K., Alexander W. D., Cole A. and Tarabad M., 1983, "Thermal Barrier Pistons and their Effect on the Performance of Compound Diesel Engine Cycles", SAE Paper 830312.

Woschni G., 1967, "A Universal Applicable Equation for the Instantaneous Heat Transfer Coefficient in the Internal Combustion Engine", SAE Paper 670931.

Yoshida Masaichi, 1983, "Heat Loss of Internal Combustion Engine". Internal Combustion Engine of Japan, Vol. 22, Mo. 284.